Electrochemical synthesis of highly corrugated graphene sheets for high performance supercapacitors
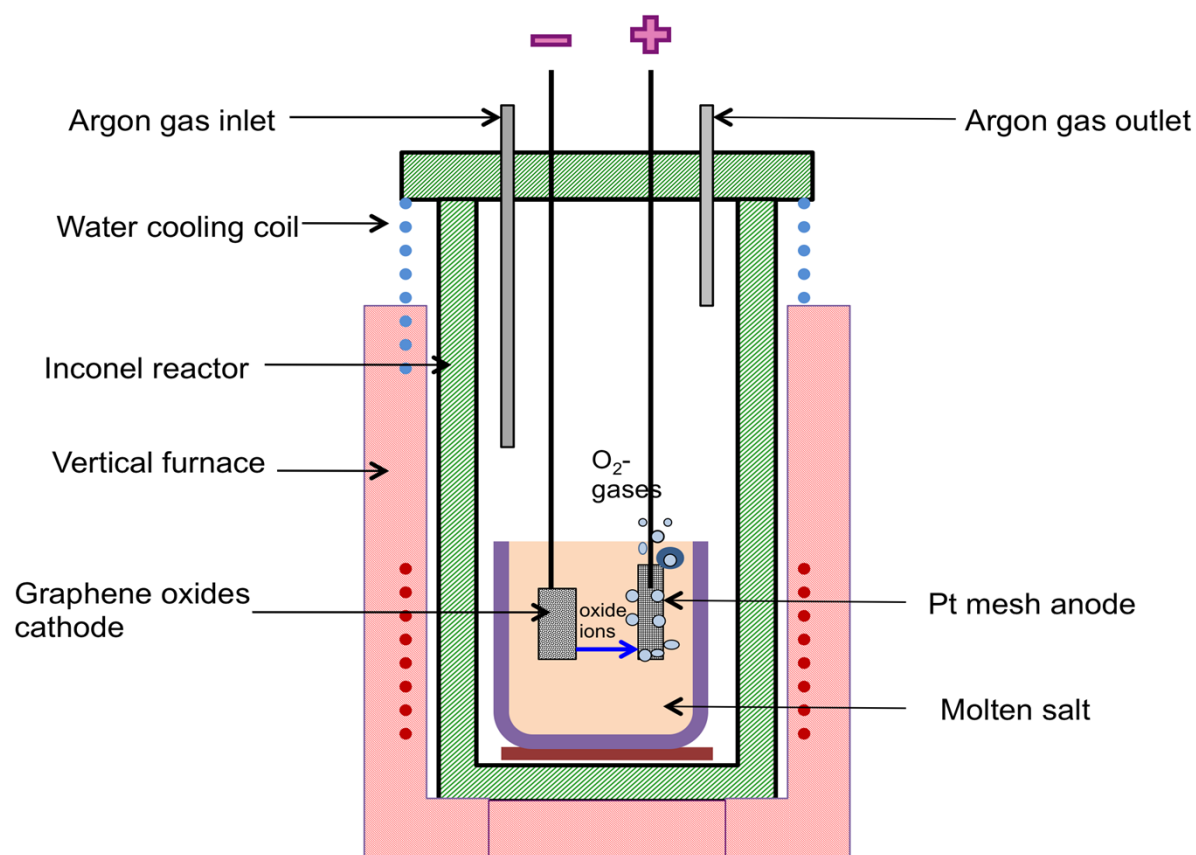
Amr M Abdelkader

Figure S1: Schematic diagram shows the electrochemical molten salt reactor used to reduce GO.

Figure S2: The stainless steel cup used as a cathode current collector. The cathode was connected to the power supply *via* stainless steel rod connected on the sidewall of the cup.
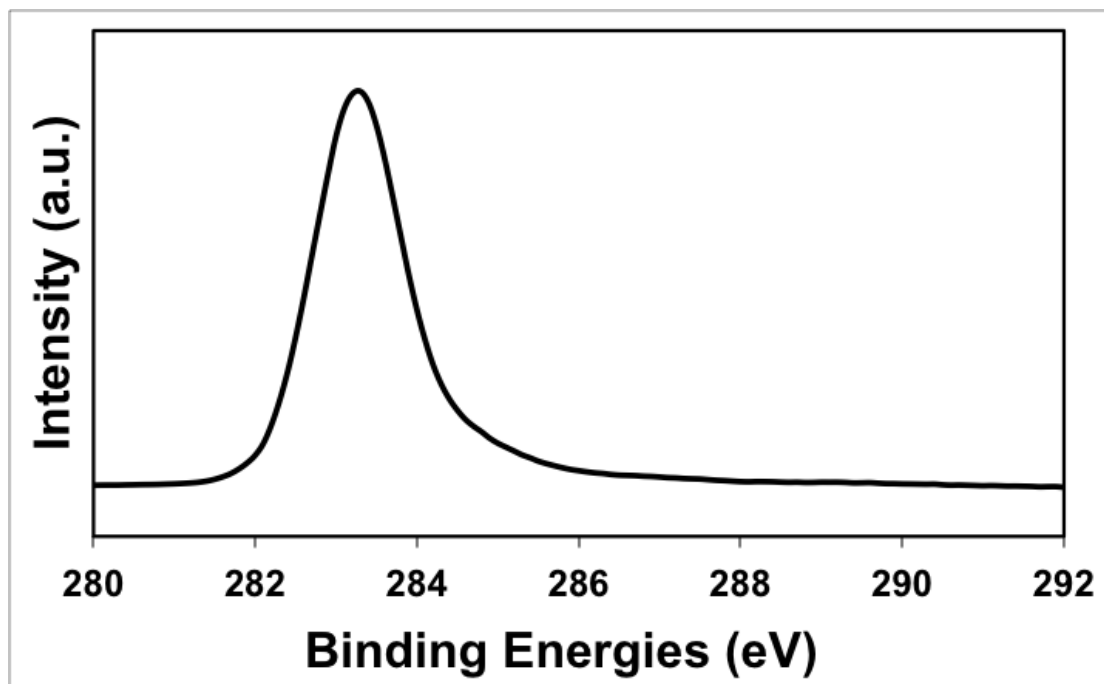

Figure S3: XPS C1 peak of the starting graphite materials. The peak is symmetrical and can be fitted with one single peak for the C-C bonds only. The C1 peaks of EDoX-GO and LiER-GO (Figure 3 in the manuscript) showed similar symmetrical shape, giving a clear evidence of an efficient process that removes the oxygen groups bonded to the carbon atoms.
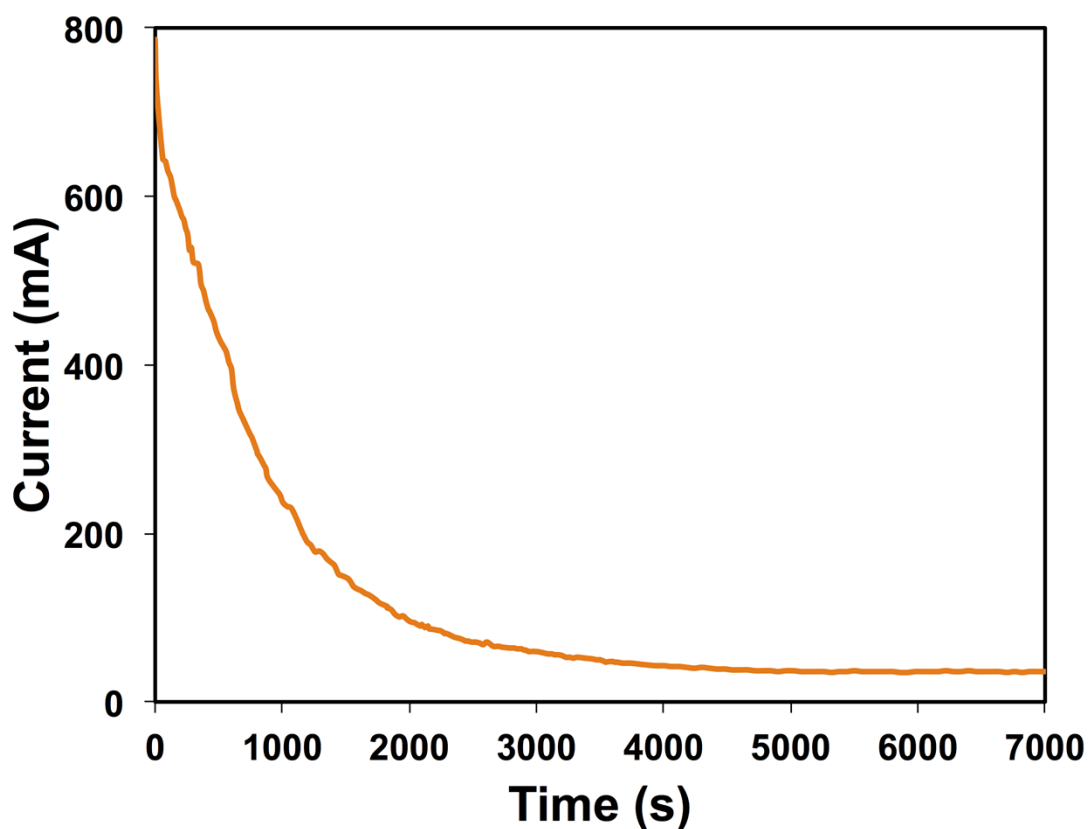
Figure S4: The time-current curve recorded during the electro-deoxidation of GO cathode at 2 V constant voltage. This chronoamperogram shows that the output current declines in the first hour following a parabolic scheme. The current for the next hour of the run is featureless and almost constant at a value of ~30 mA, indicating no electron transfer reactions were taking place. Therefore, the time of the electro-deoxidation was limited to 1 hour in the present study.

Calculating the specific capacitance obtained from CV and charge-discharge curves

From charge-discharge measurements, the specific capacitances of the rGO were obtained from the acquired data using following equation:

$$C = 4I\Delta t / m\Delta V$$

Where C represents the specific capacitances, I the constant charge current, Δt for the discharging period, m for the mass of graphene used as electrodes, ΔV for the voltage of capacitor after constant current charging.

From CV curves, the specific capacitances were calculated according to the following equation:

$$C = (\int IdV)/(vmV)$$

where I represents the current density during charging-discharging, V is the potential, v is the potential scanning rate, and m is the mass of the graphene electrodes.
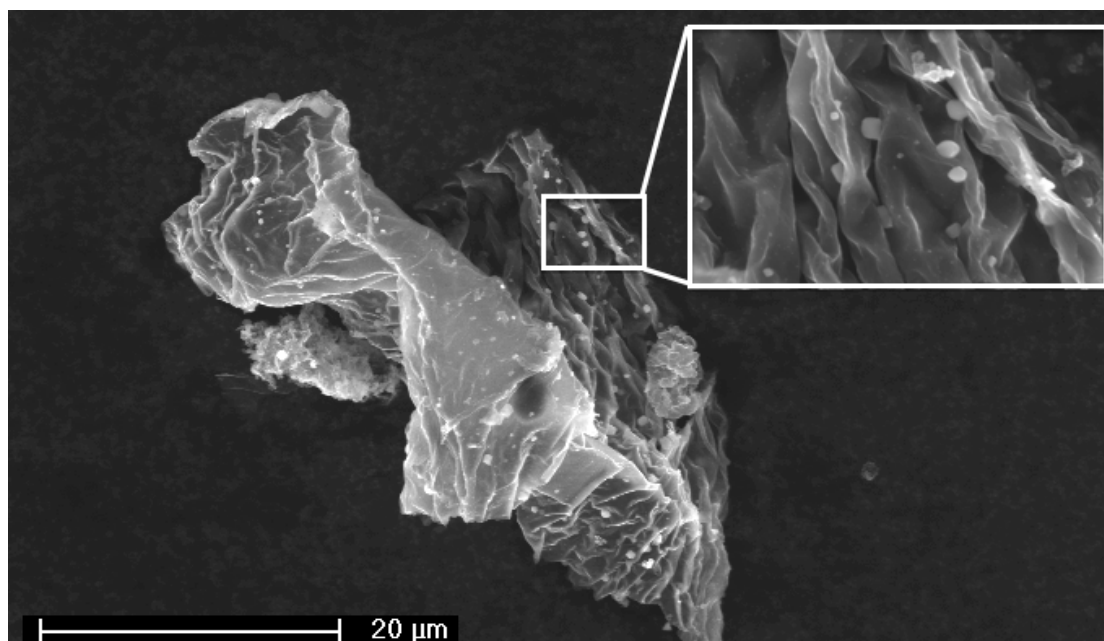

Figure S5: The molten salts trapped between the graphene flakes created a clear wavy structure upon being quenched to the room temperature.
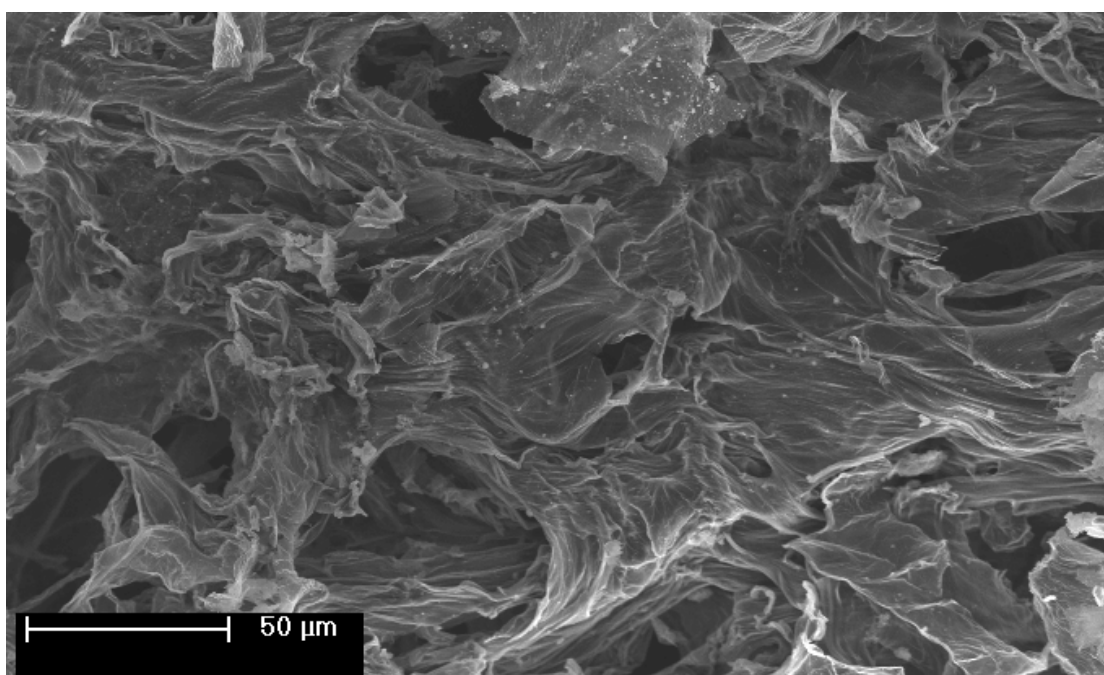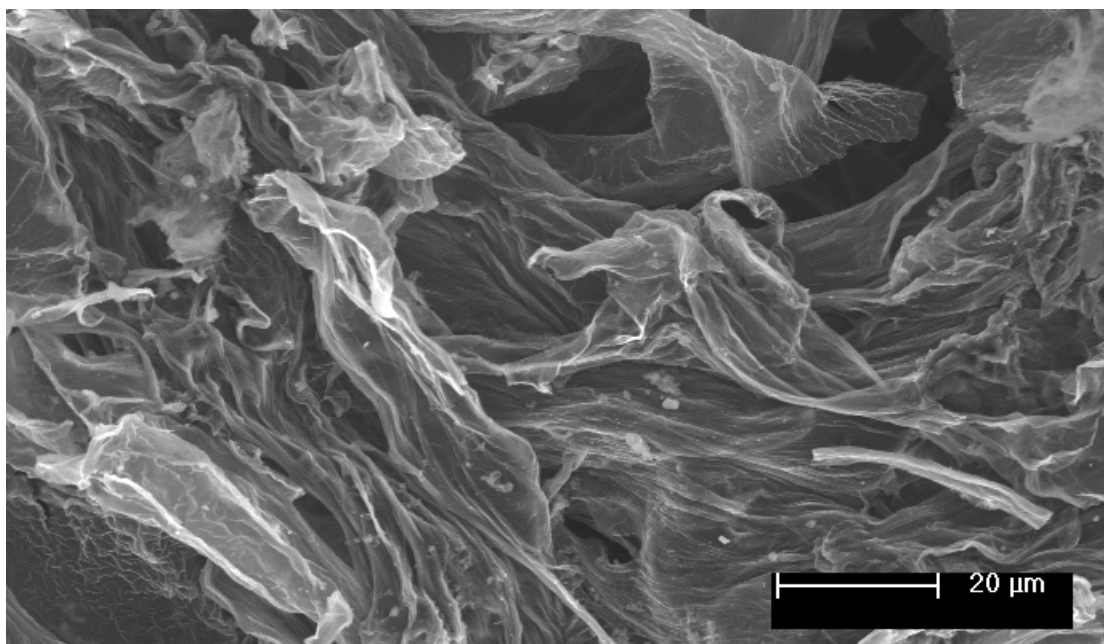
Figure S6: SEM images of the electrode fabricated using EDoX-GO at different magnifications showing the porous structure of the electrode. The individual flakes can be still identified.

Table S1: Comparison between the electrochemical reduction in molten salts and other approaches for GO reduction.

Process	Time required	C/O Ratio
Electrochemical reduction in molten LiCl-KCl under the conditions of generating Li and/or K (present work)	1 h	14.7
Direct electro-deoxidation in molten salt without the need to generate any reducing agent (present work)	1 h	12.5
Reduction in hydrazine solution at 100 °C.[1]	24 h	10.3
Reduction in pure hydrazine.[2]	One week	10.3
Hydrothermal reduction with sodium ascorbate at 95 °C.[3]	1.5	10.3
Reduction with sodium borohydride solution.[4]	2 h (thin film)	8.6
Reduction with Fe powder.[5]	6 h	7.9
Reduction with Hydrazine vapor at low pressure.[6]	72h	7.3
Reduction with alcohol.[7]	24 h	7
Reduction with Li in molten LiCl-KCl at 370 °C [8]	8	7
Hydrothermal reduction at 180 °C.[9]	6 h	5.7
Reduction with urea at 95 °C.[10]	30	4.5
Reduction with hydrobromic acid at 110 °C[11]	24	3.9
Reduction in three steps with sodium borohydride at 80 °C, aryl diazonium salt and hydrazine.[12]	27 h	N/P
Reduction of GO- Polystyrene composite with dimethylhydrazine at 80 °C.[13]	24 h	N/P
Reduction with hydrazine vapor at 40 °C and subsequently anneal at 400 °C.[1, 14]	22 h	N/P
Reduction with hydroquinone.[15]	20 h	
Thermal reduction under vacuum at 1100 °C.[14]	6 h	N/P
Reduction with hydrazine vapour.[16]	3.5h (thin film)	N/P

The electrochemical reduction and the direct electro-deoxidation in molten halide flux provide attractive alternative to reduce GO. The process is fast, and producing graphene materials with very low oxygen content as compared with other reduction methods in the literature.
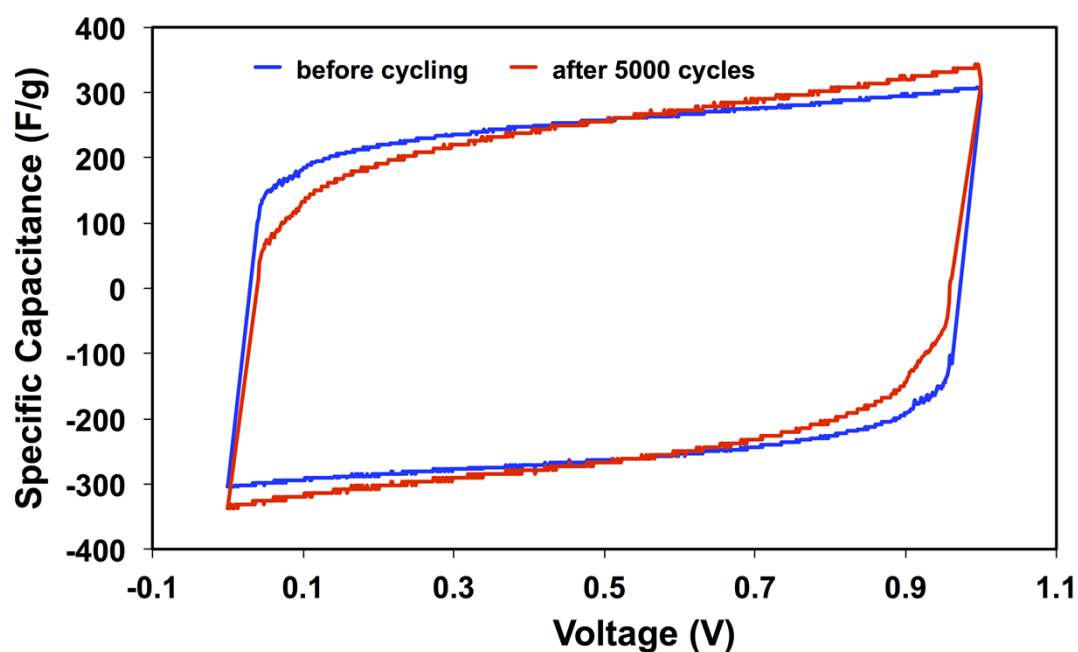
Cyclic stability of the supercapacitor

Figure S7: Comparison of the cyclic voltammograms at 80 mV/s of the supercapacitor electrode fabricated using the GO reduced *via* direct electro-deoxidation in molten salts (without the deposition of any reducing agent) before and after 5,000 cycles. Clearly, the CV maintained the rectangular shape of the original capacitor after 5,000 of galvanostatic charge/discharge cycles at 1 A/g constant current indicating that the capacitance is mainly a result of a reversible adsorption/desorption process and no irreversible pseudocapacitance was involved. The stability of the supercapacitor of the present work is amongst the highest of the graphene-based capacitors.

Supercapacitor electrode made of GO reduced under the conditions of depositing Li:
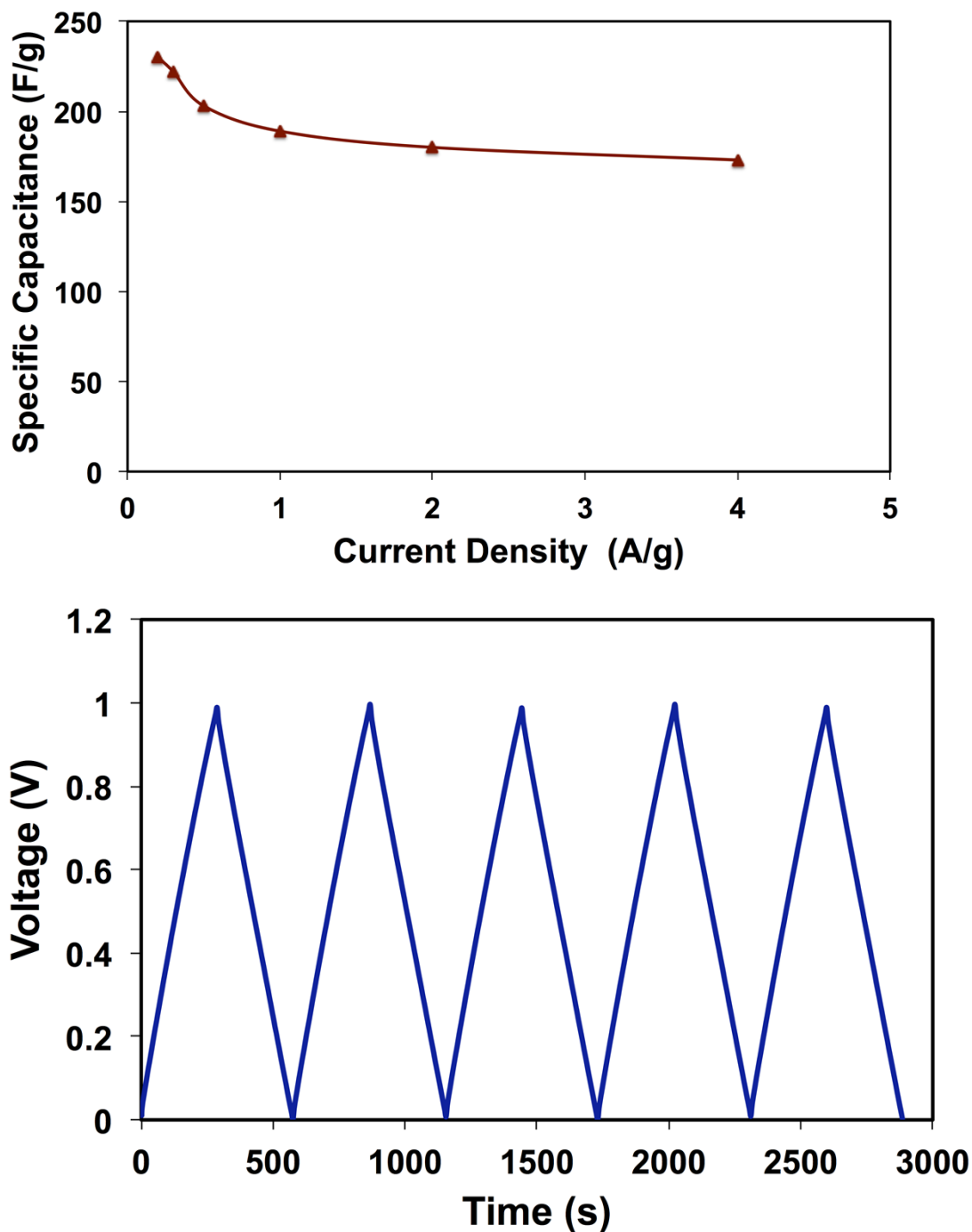

Figure S8: The electrochemical performance of the LiER-GO electrode (a) the effect of the current density on the specific capacitance as calculated from the corresponding discharge curve for each current density, and (b) the first 5 cycles of galvanostatic charge/discharge at 0.2 A/g constant current cycling.
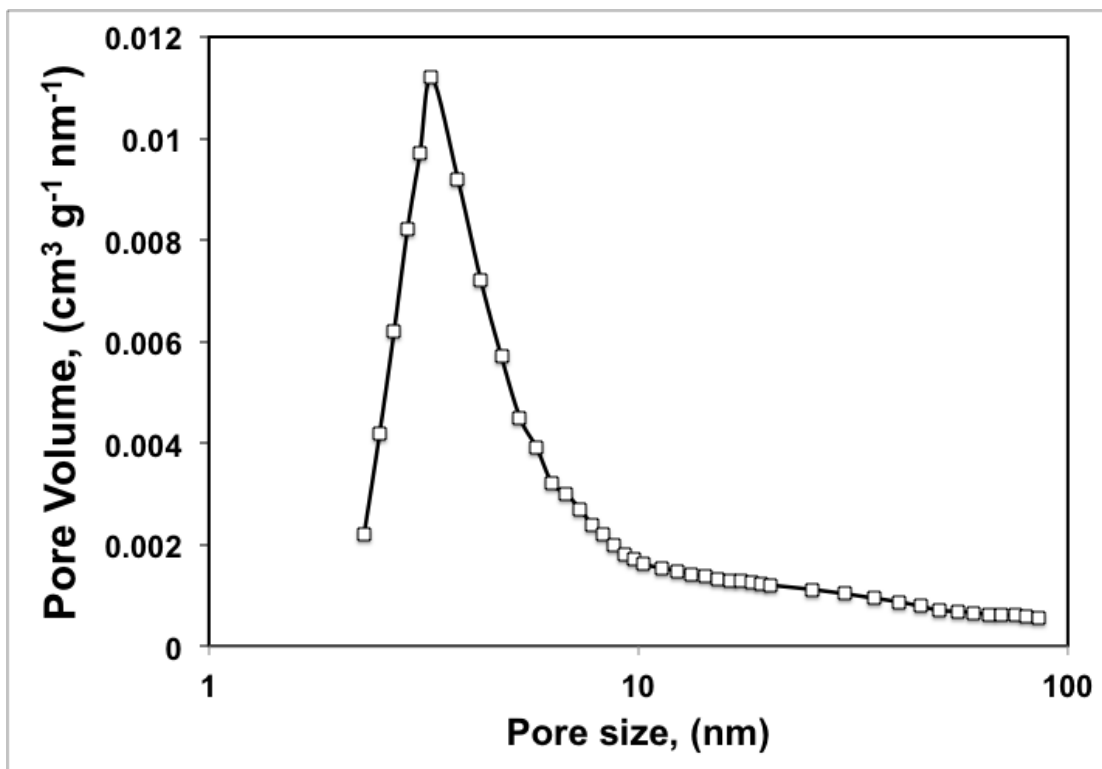
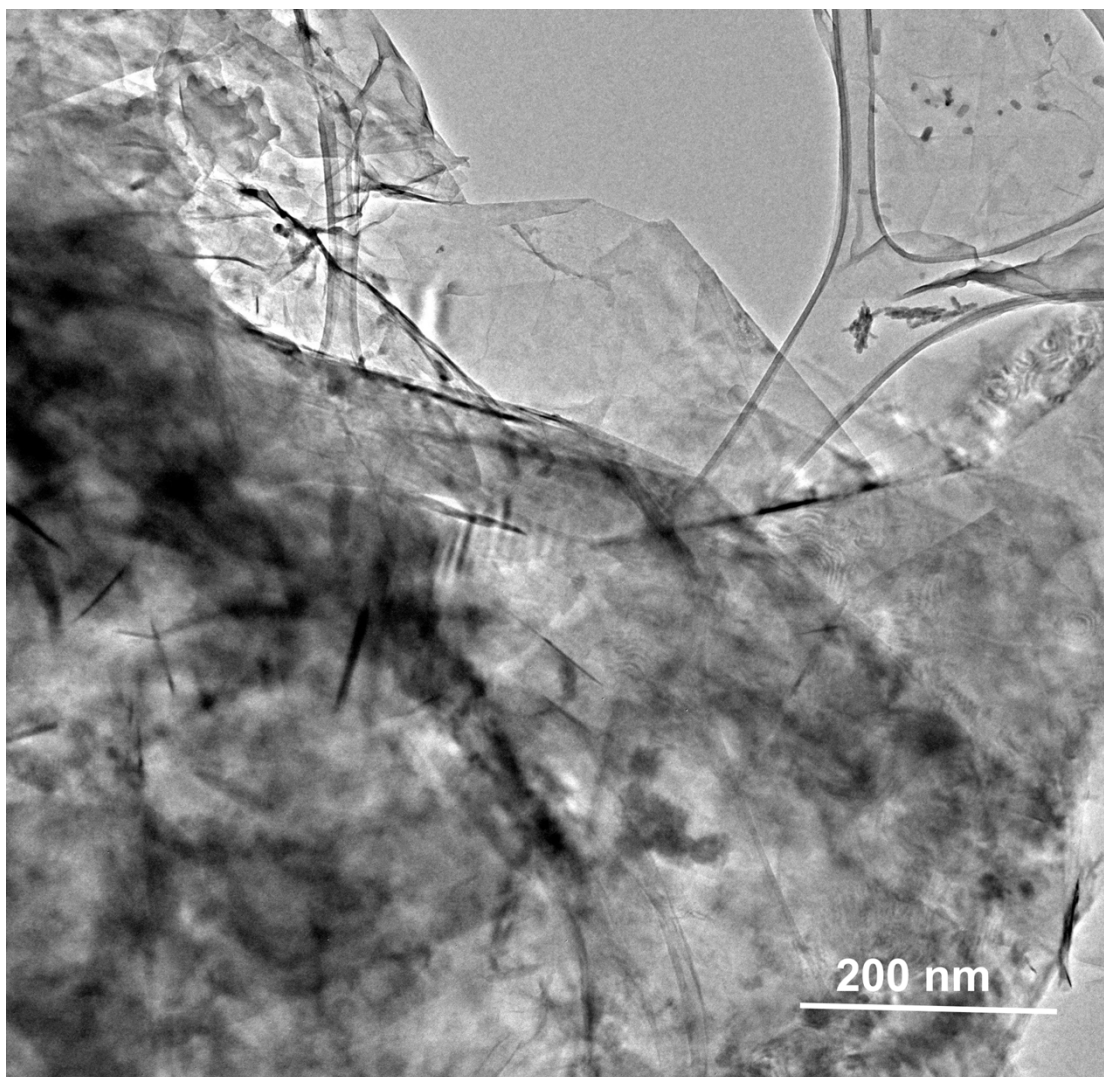Figure S9: Pore size distribution plot calculated by BJH method for the EDoX-GO sample.

Figure S10: TEM Images of the graphene powder reduced by the electrochemical reduction of GO in molten salts at 2V constant voltage.

References

1. S. Stankovich, R. D. Piner, X. Chen, N. Wu, S. T. Nguyen and R. S. Ruoff, *J. Mater. Chem.*, 2006, 16, 155-158.
2. V. C. Tung, M. J. Allen, Y. Yang and R. B. Kaner, *Nat. Nanotechnol.*, 2009, 4, 25-29.
3. K.-x. Sheng, Y.-x. Xu, C. Li and G.-q. Shi, *New Carbon Mater.*, 2011, 26, 9-15.
4. H. J. Shin, K. K. Kim, A. Benayad, S. M. Yoon, H. K. Park, I. S. Jung, M. H. Jin, H. K. Jeong, J. M. Kim, J. Y. Choi and Y. H. Lee, *Adv. Func. Materi.*, 2009, 19, 1987-1992.
5. Z.-J. Fan, W. Kai, J. Yan, T. Wei, L.-J. Zhi, J. Feng, Y.-m. Ren, L.-P. Song and F. Wei, *ACS Nano*, 2010, 5, 191-198.
6. Y. Wang, Z. Q. Shi, Y. Huang, Y. F. Ma, C. Y. Wang, M. M. Chen and Y. S. Chen, *J. Phys. Chem. C*, 2009, 113, 13103-13107.
7. D. R. Dreyer, S. Murali, Y. Zhu, R. S. Ruoff and C. W. Bielawski, *J. Mater. Chem.*, 2011, 21, 3443-3447.
8. A. M. Abdelkader, C. Vallés, A. J. Cooper, I. A. Kinloch and R. A. W. Dryfe, *ACS Nano*, 2014, 8, 11225-11233.
9. Y. Zhou, Q. Bao, L. A. L. Tang, Y. Zhong and K. P. Loh, *Chem. Mater.*, 2009, 21, 2950-2956.
10. Z. Lei, L. Lu and X. S. Zhao, *Energ. Environ. Sci.*, 2012, 5, 6391-6399.
11. Y. Chen, X. Zhang, D. Zhang, P. Yu and Y. Ma, *Carbon*, 2011, 49, 573-580.
12. Y. Si and E. T. Samulski, *Nano Lett.*, 2008, 8, 1679-1682.
13. S. Stankovich, D. A. Dikin, G. H. B. Dommett, K. M. Kohlhaas, E. J. Zimney, E. A. Stach, R. D. Piner, S. T. Nguyen and R. S. Ruoff, *Nature*, 2006, 442, 282-286.
14. H. A. Becerril, J. Mao, Z. Liu, R. M. Stoltenberg, Z. Bao and Y. Chen, *ACS Nano*, 2008, 2, 463-470.
15. G. Wang, J. Yang, J. Park, X. Gou, B. Wang, H. Liu and J. Yao, *J. Phys. Chem. C*, 2008, 112, 8192-8195.
16. S. Gilje, S. Han, M. Wang, K. L. Wang and R. B. Kaner, *Nano Lett.*, 2007, 7, 3394-3398.